

## Dynamics of defects in electroconvection patterns

This article has been downloaded from IOPscience. Please scroll down to see the full text article.

2002 Europhys. Lett. 57 824

(<http://iopscience.iop.org/0295-5075/57/6/824>)

View [the table of contents for this issue](#), or go to the [journal homepage](#) for more

### Download details:

IP Address: 148.6.26.219

The article was downloaded on 11/07/2012 at 13:24

Please note that [terms and conditions apply](#).

## Dynamics of defects in electroconvection patterns

P. TÓTH<sup>1</sup>, N. ÉBER<sup>2</sup>, T. M. BOCK<sup>1</sup>, Á. BUKA<sup>2</sup> and L. KRAMER<sup>1</sup>

<sup>1</sup> *Physikalisches Institut, Universität Bayreuth - D-95440 Bayreuth, Germany*

<sup>2</sup> *Research Institute for Solid State Physics and Optics*

*H-1525 Budapest, P.O.Box 49, Hungary*

(received 24 April 2001; accepted in final form 17 December 2001)

PACS. 61.30.Gd – Orientational order of liquid crystals; electric and magnetic field effects on order.

PACS. 61.72.Cc – Kinetics of defect formation and annealing.

PACS. 61.72.Ff – Direct observation of dislocations and other defects (etch pits, decoration, electron microscopy, X-ray topography, etc.).

**Abstract.** – In homeotropically aligned nematics with negative dielectric anisotropy the electrohydrodynamic instability occurs above a bend Fréedericksz transition. In the presence of a magnetic field  $\vec{H}$  parallel to the liquid crystal slab, ordered roll patterns with a well-defined uniform wave vector  $\vec{k}_{id}$  appear above the onset of convection. By rotating the cell around an axis perpendicular to the slab by a small angle  $\alpha$ , one can manipulate the system into a state with wave vector  $\vec{k} = \vec{k}_{id} + \Delta\vec{k}$ , where  $\Delta\vec{k}$  is roughly perpendicular to  $\vec{k}_{id}$ . We have studied experimentally the motion of defects, which then move essentially perpendicular to the rolls. The direction as well as the magnitude of the velocity as a function of  $\Delta\vec{k}$  agrees with predictions of the weakly nonlinear theory. In particular, we obtain evidence for the nonanalyticity for  $\Delta\vec{k} \rightarrow 0$ .

*Introduction.* – The structure and dynamics of topological defects in quasi-two-dimensional dissipative systems undergoing a transition to a spontaneous, stationary, periodic stripe (or roll) pattern has attracted much attention over the years [1, 2]. Here the defects are dislocations where a periodic unit (roll pair) ends or begins (positive/negative topological charge). Generally one expects the defects to move easily along the rolls (“climb”), since the (ideal, infinite) system has a continuous translational symmetry along this axis. In this way a roll pair is either added or eliminated from the system. Thus motion of defects represents a mechanism for change, and possibly selection of the wavelength, which can typically take on values within a band bounded by secondary instabilities.

Similarly, motion of defects perpendicular to the rolls (“glide”) changes the orientation of the roll pattern. Thus, such motion can provide a mechanism for selection of the orientation. This, however, is relevant only in systems with an externally imposed anisotropy. Also, since the displacement of a defect across the rolls does not correspond to a continuous translational symmetry of the system, the orientation selection is not necessarily perfect, *i.e.* the pattern provides some pinning against glide.

Near the threshold of the primary instability leading to the periodic pattern (we assume a supercritical bifurcation) these general concepts can be made explicit by using the weakly

nonlinear description in terms of universal amplitude equations. In anisotropic situations this is the (real) Ginzburg-Landau equation (GLE), which can be derived from a minimizing potential [3]. Also, in this regime, the selection of the orientation is expected to become essentially perfect because spatial variations of the amplitude then become slow on the scale of the wavelength of the pattern, which eliminates pinning. Accordingly, at given value(s) of the control parameter(s) one has an ideal (“background”) wave vector  $\vec{k}_{id}$  corresponding to the potential minimum where isolated defects do not move (“band center”). For nonzero background wave vector mismatch  $\Delta\vec{k} = \vec{k} - \vec{k}_{id}$ , defects are expected to move perpendicular to  $\Delta\vec{k}$  in a way that  $|\Delta\vec{k}|$  decreases. The relation of the velocity  $v$  *vs.*  $|\Delta\vec{k}|$  obtained from the GLE is nonlinear. In particular, it involves a weak (logarithmic) nonanalyticity for  $\Delta k \rightarrow 0$  [2, 4, 5].

Electroconvection (EC) in *planarly aligned* nematic liquid crystals (LCs) is the prime example for anisotropic convection [6]. Here the preferred axis is fixed by the direction of surface anchoring of the director  $\hat{\mathbf{n}}$  describing the average molecular orientation of the LC. In the normal-roll regime  $\vec{k}_{id} \parallel \hat{\mathbf{n}}$ . The predictions described above regarding the direction of motion and the order of magnitude of the speed were verified in early experiments with the background wave vector controlled (within some limits) by structured electrodes [7]. At the same time, good overall semi-quantitative agreement was found in experiments on the same system with the wave number controlled by making use of the frequency dependence of the critical wave number [8, 9]. This method limited the accessible mismatch to changes of the background wavelength, *i.e.*  $\Delta\vec{k} \parallel \vec{k}_{id}$ , which only induces climb. Also, large negative mismatch of the wave number was excluded. Most importantly, the region of small  $\Delta k$  could not be resolved accurately, presumably because of the presence of other defects, which introduce a cutoff of the singularity. Thus, the nonanalytic behavior for  $\Delta k \rightarrow 0$  could not be verified. In fact, the results could not discriminate against a theory presented in [8] where an *ad hoc* gauge field was introduced to provide a cutoff for the nonanalyticity. This limitation was overcome in recent work by introducing controlled creation of defect pairs by a laser beam [10]. The resulting velocity curves gave evidence for the nonanalytic behavior.

*Homeotropically aligned* nematic LCs, on the other hand, where EC appears above a bend Fréedericksz transition, offer the possibility to control the anisotropy by an additional planar magnetic field  $\vec{H}$  [11]. In fact, the preferred axis can be varied by rotating  $\vec{H}$  with respect to the sample *after* the pattern has formed. Thus a mismatch leading predominantly to glide can be introduced in a very convenient and accurate way. In this paper we present experiments in this system, which, for the first time, give quantitative results on glide. The results clearly exhibit the curvature of  $v(|\Delta\vec{k}|)$  demonstrating the logarithmic nonanalyticity for  $\Delta k \rightarrow 0$  for the case of glide motion.

*Experimental setup.* – Two of the usual capacitor-type cells were used with a thin slab of nematic ( $x$ - $y$  plane) sandwiched between two glass plates coated with transparent electrodes (ITO). The plates were separated by spacers, which determined the thickness of the LC layer  $d$  as  $27\mu\text{m}$  (cell  $c1$ ) and  $79.5\mu\text{m}$  (cell  $c2$ ), respectively. The area of the cell was of the order of  $1\text{ cm} \times 1\text{ cm}$ . Homeotropic anchoring of the director was achieved by coating the inner surfaces of the plates with a layer of the surfactant dimethyloctadecyl [3-(trimethoxysilyl)-propyl]ammonium chloride. The cells were filled, respectively, with the nematic materials Phase 5A (Merck) ( $c1$ ) and MBBA mixed with 0.16% wt. of a blue anthraquinone dye (D16 from BDH) ( $c2$ ). For the parameters of the LC materials, see [12]. The cells have been sealed in order to avoid aging effects in the LC materials. In fact, their conductivity remained fairly constant during the experiments.

An ac voltage (rms voltage  $V$ , frequency  $f$ ) was applied across the LC slab ( $\parallel z$ ) by a PC-driven function generator. Additionally, a magnetic field  $\vec{H}$  was applied in the  $x$ -direction,

which tends to align the director parallel to it. The value of the magnetic induction was 103 mT, which corresponds to  $0.27H_F$  (where  $H_F$  is the magnetic bend Fréedericksz threshold) in the case of  $c1$  and to  $0.88H_F$  in that of  $c2$ . The cell was mounted on a holder, which could be rotated by a stepper motor around the  $z$ -direction by  $1.54^\circ$  per step.

The temperature of the LC cell was stabilized at  $25.0 \pm 0.1^\circ\text{C}$  by a thermostated water circuit.

An area of the cell up to  $1\text{ mm}^2$  was observed by means of a long-range microscope with working distance of about 30 cm. The convection pattern was visualized by the shadowgraph method [13] in light polarized parallel to  $\vec{H}$  passing the cell in the  $z$ -direction. A CCD camera was mounted onto the microscope and connected to a frame grabber card that digitized the images with a spatial resolution of  $512 \times 512$  pixels and 256 gray scales.

The measurements of the defect motion were performed at 850 Hz, 8.17 V ( $\epsilon = V^2/V_c^2 - 1 = 0.031$ ) for cell  $c1$  and at 1050 Hz, 14.05 V ( $\epsilon = 0.028$ ) for cell  $c2$ . This was well within the range of stable normal rolls, which towards low frequencies is bounded by the Lifshitz point  $f_L, V_L$  (crossover to oblique rolls at threshold) and towards high frequencies by the crossover to the dielectric range at  $f_{cr}, V_{cr}$  [6]. We had  $f_L = 645\text{ Hz}$ ,  $V_L = 7.48\text{ V}$  and  $f_{cr} = 1952\text{ Hz}$ ,  $V_{cr} = 62.41\text{ V}$  for cell  $c1$ , and  $f_L = 875\text{ Hz}$ ,  $V_L = 11.77\text{ V}$ ,  $f_{cr} \cong 2500\text{ Hz}$ ,  $V_{cr} \cong 100\text{ V}$  for cell  $c2$ . By increasing the voltage the transition to abnormal rolls [14] sets in at 8.35 V, *i.e.*  $\epsilon = 0.077$  ( $c1$ ), and 14.6 V, *i.e.*  $\epsilon = 0.11$  ( $c2$ ), respectively.

*Experimental methods.* – Initial states with well-isolated defects in a rotated cell were created by two methods:

i) A voltage jump from a negative  $\epsilon$  to a positive value into the defect turbulent range ( $\epsilon \approx 0.2$ ) led to the creation of a large number of defects. This was followed by another jump to the measuring voltage, where defects annihilated. We waited until one defect was found near the rotation axis of the cell, separated from other defects by at least  $500\mu\text{m}$ . Then the cell was rotated. This method was applied to  $c1$  as well as to  $c2$ .

ii) Exclusively in cell  $c2$  another method was also applied, which created only one pair of defects at a chosen position [10]. The beam of a He-Ne laser of 0.1 mW power was focussed to the middle of the cell heating up the LC locally without disturbing the observation of the patterns. The spot size was of about the period of the pattern (a roll pair). The blue dye enhanced the absorption of the beam energy which could be regulated by filters. Heating reduces  $V_c$ , thus  $\epsilon$  was increased locally, which quickly led to the creation of a pair of defects, see fig. 1(a). The laser was switched off and after the rotation the defects started to move in opposite direction, if  $|\alpha|$  was large enough and the appropriate sense of rotation was chosen. In case the desired mismatch was too small to drive the two defects apart, initially a larger  $\alpha$  was applied in order to separate the defects; subsequently the cell was rotated back to the chosen angle for the measurement.

After the rotation the system relaxed rapidly to a state with the adjusted background wave vector  $\vec{k}$  away from  $\vec{k}_{id} \parallel \vec{H}$ , which induced the defect motion as a mechanism to reduce the mismatch. Relaxation of the defect into its final constant-velocity configuration is slower. The procedure was carried out for defects of both topological charges and rotations in both senses by angles  $|\alpha| = n \times 1.54^\circ$  with  $0 < n \leq n_f$ . The upper limit  $n_f$  can be associated with the Eckhaus stability limit of the patterns (see below). It was 6 and 9 for cells  $c1$  and  $c2$ , respectively. Exceeding this limit slightly led rapidly to a spontaneous creation of defects. Also within the Eckhaus stable range [15,16] there was a slow relaxation towards  $\vec{k}_{id}$ , which we attribute to the creation of defects at inhomogeneities. Although for larger  $n$  the relaxation was faster, there remained, for  $n < n_f$ , a time window for measuring the defect velocity. Figure 1(b) shows a defect after the rotation of the cell. Also shown is  $\vec{k}_{id}$  together with the actual

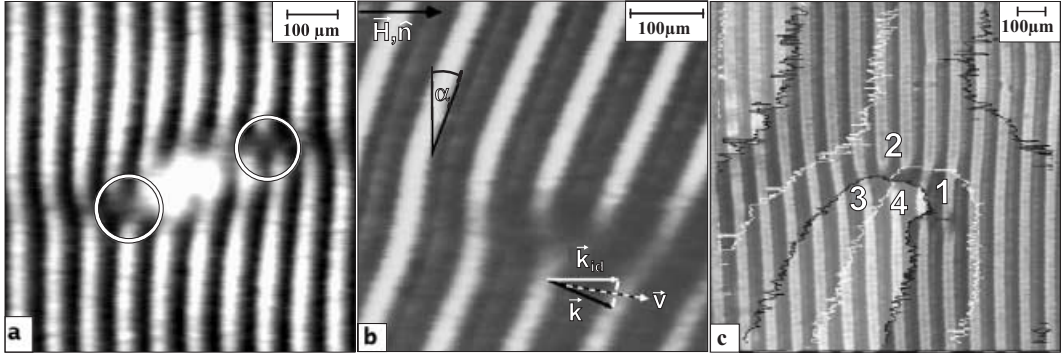


Fig. 1 – Snapshots of  $c2$  (different magnifications). a) Creation of a defect pair (encircled) by a laser beam (bright spot); b) single defect after rotation of the cell; c) extracting the position of a defect from the phase  $\phi$  of the demodulated complex amplitude  $A_d$ . Equiphase lines are superposed on the underlying pattern; white lines:  $\text{Re}(A_d) = 0$ ; black lines:  $\text{Im}(A_d) = 0$ ; region 1:  $0 < \phi < \pi/2$ , region 2:  $\pi/2 < \phi < \pi$ , region 3:  $\pi < \phi < 3/2\pi$ , region 4:  $3/2\pi < \phi < 2\pi$ . The defect is located where the white and the black lines cross.

wave vector  $\vec{k}$  and the expected direction of the velocity  $\vec{v}$  of the defect perpendicular to the mismatch  $\Delta\vec{k}$ . One has  $|\Delta\vec{k}| = 2|\vec{k}_{id}|\sin(\alpha/2)$ .

The location of the defect was determined by a demodulation method described in [17] (see fig. 1(c)), which is an extension of the method used in [8–10] to two dimensions, for a sequence of times separated by intervals  $\Delta t$  chosen between 40 and 15000 ms. The measurement was stopped when the direction of the rolls as determined from a two-dimensional FFT with an accuracy of  $0.95^\circ$  for  $c1$  and  $1.32^\circ$  for  $c2$ , was detected to have changed or other defects came too near. Figure 2(a) shows examples of trajectories of defects with positive charge for three angles  $\alpha$  ( $x$ -axis parallel to  $\vec{H}$ ). The motion of the defects is (on average) mostly glide (note

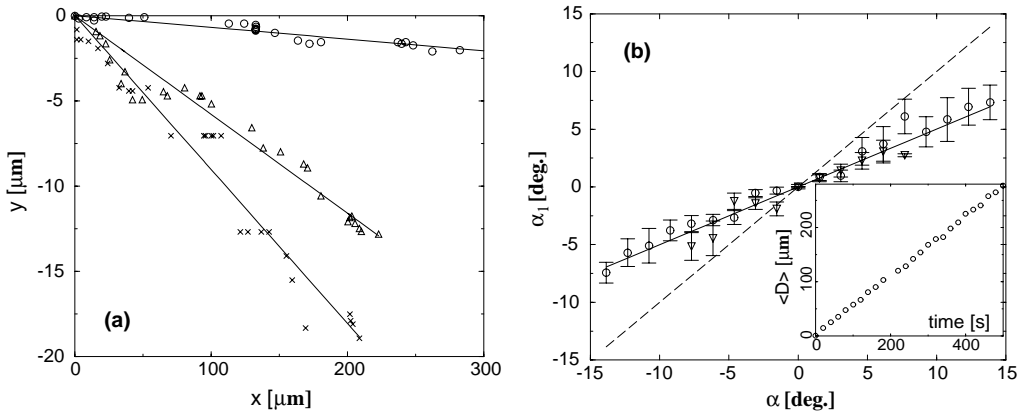


Fig. 2 – a) Examples of defect trajectories with linear fits for cell  $c2$ . Circles:  $\alpha = 3.08^\circ$ ,  $\Delta t = 20$  s; triangles:  $\alpha = 6.16^\circ$ ,  $\Delta t = 10$  s; crosses:  $\alpha = 10.78^\circ$ ,  $\Delta t = 10$  s; b) average direction of motion of the defect as determined from linear fits. Triangles: cell  $c1$ ; circles: cell  $c2$ . The solid line denotes the relation between  $\alpha_1$  and  $\alpha$  corresponding to  $\vec{v} \perp \Delta\vec{k}$ ; the dashed line denotes simple glide motion. Insert: the displacement  $\langle D \rangle$  of a defect *vs.* time averaged over many runs for cell  $c2$ ,  $\alpha = 3.08^\circ$ .

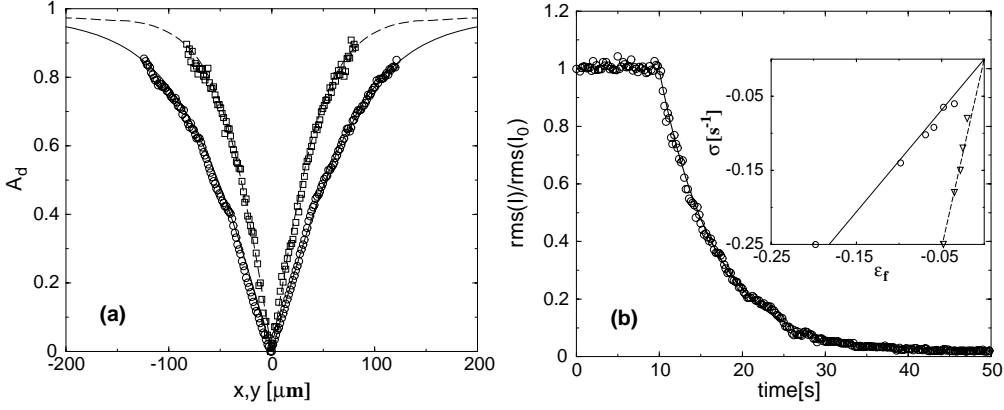


Fig. 3 – Determination of the parameters of the GLE for cell c2. a) Demodulated normalized amplitude  $|A_d|$  of a defect parallel (circles) and perpendicular (squares) to  $\vec{k}$ . The fit curves provide  $\xi_{\parallel}$  and  $\xi_{\perp}$ . b) Decay of contrast for  $\epsilon_f = -0.1$  with an exponential fit  $\exp[\sigma t]$ . Insert: decay rates  $\sigma$  vs.  $\epsilon_f$  giving  $\tau_0^{-1} = \sigma/\epsilon_f$  (dashed line: cell c1, solid line: cell c2).

the different scales for  $x$  and  $y$ ). The velocity  $\vec{v}$  obtained by dividing the displacements by  $\Delta t$  exhibits a modulation which results from the defects crossing the roll pattern in their glide motion. To remove this modulation, the speed  $|\vec{v}|$  was averaged over the trajectory. The mean direction of  $\vec{v}$  was estimated by fitting to the discretized trajectory (actually, a linear fit turned out to be sufficient) defining an angle  $\alpha_1$  with respect to  $\vec{H}$ . In this way averaged values for  $|\vec{v}|$  and  $\alpha_1$  for a run with fixed  $\Delta\vec{k}$  were determined. This whole procedure was repeated at least ten times with averaging over subsequent runs (altogether at least 300 space-time coordinates contributed to the determination of the velocity for each  $\Delta\vec{k}$ ). This was necessary in order to smooth out the inherent modulation of the velocity due to pinning to the roll pattern (see fig. 2(a)). The efficiency of this technique is illustrated in the insert in fig. 2(b) which shows the time evolution of the distance  $\langle D \rangle$  of a defect from its initial position averaged over several runs. Since pinning is absent in the case of pure climb, trajectories are smoother and this kind of averaging over many runs was not necessary there [8–10]. The error bars shown in the results below represent the rms standard deviations of the different runs.

*Results and discussion.* – The angle  $\alpha_1$  which defines the (averaged) direction of motion of the defects with respect to  $\vec{H}$  is plotted against  $\alpha$  in fig. 2(b). The direction of the motion was found to be perpendicular to  $\Delta\vec{k}$ , as expected from the theory. For given  $\alpha$  defects of opposite charge moved in opposite directions.

The theoretical prediction for the absolute value of the velocity  $vs.$  mismatch as obtained from the GLE is given by [4, 5]

$$\mathcal{V} \ln(V_0/\mathcal{V}) = 2K(1 - 0.35K^2), \quad (1)$$

with the scaled velocity  $\mathcal{V} = \frac{\tau_0}{\sqrt{\epsilon}} \sqrt{(v_x^2/\xi_{\parallel}^2 + v_y^2/\xi_{\perp}^2)}$ , mismatch  $K = \frac{1}{\sqrt{\epsilon}} \sqrt{(\Delta k_x^2 \xi_{\parallel}^2 + \Delta k_y^2 \xi_{\perp}^2)}$ , and  $V_0 = 3.29$ . Note the logarithmic singularity at  $K = 0$ .

In order to compare with the experiments, it is necessary to determine the coherence lengths  $\xi_{\parallel}$  and  $\xi_{\perp}$  of the pattern as well as the correlation time  $\tau_0$  (extrapolated to  $\epsilon = 1$ ). The first were determined by a fit of the demodulated amplitude  $|A_d|$  for a static defect ( $\alpha = 0$ ) to a corresponding numerical solution of the GLE [4] (see fig. 3(a)). The values of the

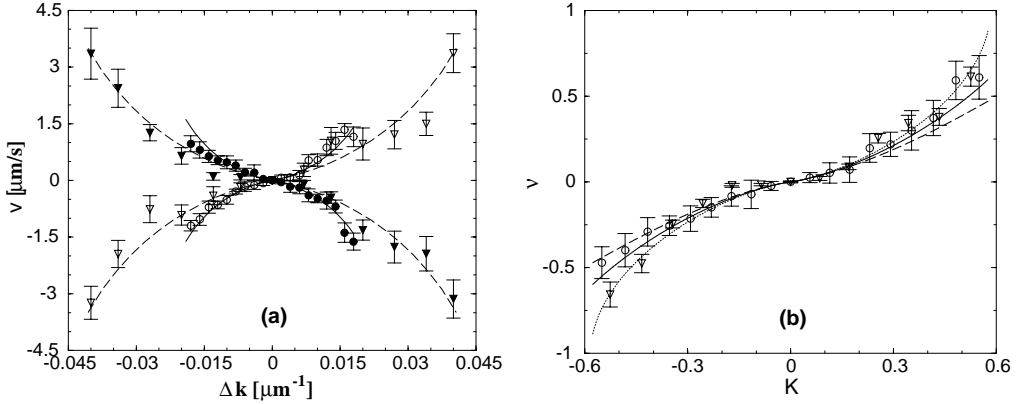


Fig. 4 – a) Comparison between experiment (symbols) and theory (lines) of the velocity  $v$  *vs.* mismatch  $\Delta k$  for defects with positive and negative charge (empty and full symbols, respectively) in cell  $c1$  (triangles/dashed lines) and  $c2$  (circles/solid lines). b) Same data, but average of absolute value for positive and negative defects in dimensionless units. The theory (eq. (1)) is given by the solid curve. The other curves are obtained from eq. (1) with altered values of  $V_0$  (dashed:  $V_0 = 4.1$ , dotted  $V_0 = 2.9$ ).

coherence lengths averaged over ten defects were  $\xi_{\parallel}/d = 0.17 \pm 0.03$  and  $\xi_{\perp}/d = 0.09 \pm 0.02$  for  $c1$ , and  $\xi_{\parallel}/d = 0.12 \pm 0.02$  and  $\xi_{\perp}/d = 0.07 \pm 0.02$  for  $c2$ . The correlation time was determined by recording the decay of the contrast of the pattern at band center after a jump from a small positive  $\epsilon$  ( $\leq 0.02$ ) to various negative values  $\epsilon_f$  and fitting it to the function  $\exp[\sigma t]$  with  $\sigma = \epsilon_f/\tau_0$ . Figure 3(b) shows an example of this fit and plots (insert) of  $\sigma$  *vs.*  $\epsilon_f$  for both cells (performing the fit with the full decay function of the GLe leads to insignificant corrections). We obtain  $\tau_0 = 0.191 \pm 0.021$  s for  $c1$  and  $\tau_0 = 0.717 \pm 0.075$  s for  $c2$ . The parameters are near to the theoretical results given in ref. [12] for planar MBBA for a comparable frequency, namely  $\xi_{\parallel} = 0.25$ ,  $\xi_{\perp} = 0.13$ , and  $\tau_0/d^2 = 0.11$  ms/ $(\mu\text{m})^2$ .

The final results are shown in fig. 4. In fig. 4(a)  $v$  is plotted *vs.* the magnitude of  $\Delta \vec{k}$  for both cells distinguishing between the two topological charges. The theoretical curves were calculated from eq. (1) using the measured parameters  $\xi_{\parallel}$ ,  $\xi_{\perp}$ , and  $\tau_0$ . Finally, in fig. 4(b), all data are plotted in the dimensionless units, where they collapse —within error— to a single curve. Clearly the theoretical curve provides a much better fit (in particular for small  $|\Delta \vec{k}|$ ) than a linear relation between velocity and wave vector mismatch. In order to assess the quality of the comparison between the experiment and the theory, we have included two curves obtained from eq. (1) with the theoretical value 3.29 of  $V_0$  replaced by 4.1 (dashed) and 2.9 (dotted), respectively.

This then is a strong indication for the existence of the logarithmic nonanalyticity at  $\Delta k \rightarrow 0$  (as found also for climb in planar cells [10]). The logarithmic singularity is a signature of the long-range deformation field surrounding a defect resulting from the diffusive behavior of the phase in 2D. Its appearance is not restricted to the weakly nonlinear regime. The results provide experimental evidence against the *ad hoc* theory presented in [8]. A cutoff of the singularity is introduced by the system size or the distance to other defects.

*Concluding remarks.* – With the experiments presented here it was possible to measure the velocity *vs.* wave vector mismatch curve in the full Eckhaus stable range for predominant glide motion. Though modulations of the velocity, which arise from the motion across the

underlying patterns were clearly detected, the averaged velocities behaved according to the predictions of the weakly nonlinear theory. Particularly good resolution could be achieved by using a relatively thick cell, which made it possible to demonstrate the nonlinear dependence of the velocity on the mismatch.

\* \* \*

The authors thank V. STEINBERG, R. BENITEZ and I. JÁNOSSY for fruitful discussions, and I. JÁNOSSY additionally for technical support. P. TÓTH acknowledges the hospitality of the Research Institute for Solid State Physics and Optics (Budapest). Financial support by the DFG through Kr690/13-1, the Hungarian Research Grant No. OTKA-T031808, and EU through TMR network FMRX-CT96-0085 is gratefully acknowledged.

## REFERENCES

- [1] CROSS M. C. and HOHENBERG P. C., *Rev. Mod. Phys.*, **65** (1993) 851.
- [2] PISMEN L. M., *Vortices in Nonlinear Fields* (Oxford Science Publications) 1999.
- [3] PESCH W. and KRAMER L., *Z. Phys.*, **63** (1986) 121.
- [4] BODENSCHATZ E., PESCH W. and KRAMER L., *Physica D*, **32** (1988) 135; KRAMER L., BODENSCHATZ E., PESCH W., THOM W. and ZIMMERMANN W., *Liq. Cryst.* **5** (1989) 699; KRAMER L., BODENSCHATZ E. and PESCH W., *Phys. Rev. Lett.*, **64** (1990) 2588; WEBER A., BODENSCHATZ E. and KRAMER L., *Adv. Mater.*, **4** (1991) 191; BODENSCHATZ E., WEBER A. and KRAMER L., *J. Stat. Phys.*, **64** (1991) 1007.
- [5] PISMEN L. M. and RODRIGUEZ J. D., *Phys. Rev. A*, **42** (1990) 2471.
- [6] KRAMER L. and PESCH W., in *Pattern Formation in Liquid Crystals*, edited by BUKA A. and KRAMER L. (Springer, Berlin) 1995.
- [7] NASUNO S., TAKEUCHI S. and SAWADA Y., *Phys. Rev. A*, **40** (1989) 3457.
- [8] GOREN G., PROCACCIA I., RASENAT R. and STEINBERG V., *Phys. Rev. Lett.*, **63** (1989) 1237.
- [9] RASENAT S., STEINBERG V. and REHBERG I., *Phys. Rev. A*, **42** (1990) 5998.
- [10] ILAN D. and STEINBERG V., unpublished (1996); ILAN D., M. SC. Thesis, Weizmann Institute, Rehovot, 1996.
- [11] RICHTER H., KLÖPPER N., HERTRICH A. and BUKA Á., *Europhys. Lett.*, **30** (1995) 37.
- [12] BODENSCHATZ E., ZIMMERMANN W. and KRAMER L., *J. Phys. (Paris)*, **49** (1988) 1875; TREIBER M., ÉBER N., BUKA Á. and KRAMER L., *J. Phys II*, **7** (1997) 649.
- [13] RASENAT S., HARTUNG G., WINKLER B. and REHBERG I., *Exp. Fluids*, **7** (1989) 412.
- [14] RICHTER H., BUKA Á. and REHBERG I., in *Spatio-temporal patterns in nonequilibrium complex systems, Santa Fe Institute Studies in the Sciences of Complexity*, Vol. **XXI**, edited by CLADIS P. and PALFFY-MUHORAY P. (Addison-Wesley, New York) 1994; PLAUT E., DECKER W., ROSSBERG A., KRAMER L., PESCH W., BELAIDI A. and RIBOTTA R., *Phys. Rev. Lett.*, **79** (1997) 2376; HUH J.-H., HIDAKA Y. and KAI S., *Phys. Rev. E*, **58** (1998) 7355; RUDROFF S., ZHAO H., KRAMER L. and REHBERG I., *Phys. Rev. Lett.*, **81** (1998) 4144; ROSSBERG A. G., ÉBER N., BUKA Á. and KRAMER L., *Phys. Rev. E*, **61** (2000) R25.
- [15] RASENAT S., BRAUN E. and STEINBERG V., *Phys. Rev. A*, **43** (1991) 5728.
- [16] NASUNO S. and KAI S., *Europhys. Lett.*, **14** (1991) 779.
- [17] SCHEURING M., KRAMER L. and PEINKE J., *Phys. Rev. E*, **58** (1998) 2018.